

MagNet Challenge 2023 Final Report

Chushan Li, *Member, IEEE*, Yinan Yao, *Student Member, IEEE*, Tianxiang Hu, *Student Member, IEEE*,
Lumeng Xu, Yiyi Wang, Sichen Wang

Abstract- Modeling of magnetic material loss is fundamental in magnetic components design, yet no fully satisfactory model has been proposed due to the complexity of underlying physics. Equation based model can not guarantee precise results across the entire application range. Data driven model is expected to surpass the limitations of equation-based method, but current research still faces challenges in terms of model size, accuracy, and the applicability range. Therefore, a physics informed neural network (PINN) model with smaller size, higher accuracy, wide applicability range and reduced data dependency is proposed. The improved general Steinmetz equation is incorporated into NN for mitigation of model reliance on extensive datasets. The architecture of the proposed model combines Gated Recurrent Unit and Feedforward Neural Network, enabling the seamless integration of waveform, temperature, and frequency information within a unified framework. The proposed model has compact size of 4285 parameters, and achieves 95-prct error of 8.35%, 4.11%, 8.78%, 25.70%, and 8.74% for new materials A, B, C, D, E. Notably, the model exhibits reduced data dependency, as it achieves comparable accuracy with only 25 data points, whereas normal NN model that doesn't incorporate physics information require more than 300 data points for acceptable performance.

I. INTRODUCTION

Magnetics components, which are transformers and inductors, are widely used in power electronics systems for energy storage, energy conversion and electrical isolation, etc. Typical magnetic components occupy large volume of the power electronics system and has high power loss, thus limiting the improvement of efficiency and power density of the whole system. Establishing an accurate magnetics loss model is crucial for effective material selection, thermal design, and performance prediction of magnetic components, which provides essential guidance to the overall system design and optimization.

Magnetic material has complicated physical mechanism, which is the first main difficulty of core loss modeling. Also, due to the frequency varying, temperature varying and dc bias varying characteristics of the high permeability magnetic material, the loss model is a highly nonlinear system, which adds difficulty to the core loss modeling. Furthermore, factors including frequency, temperature and dc bias are coupled and changing together in real conditions, therefore adding complexity to characterizing magnetics materials[1].

Currently, there is no universally applicable and accurate physical formula for magnetic loss. Models based on physical mechanisms are complex and demand extensive experimental data, making them impractical for real-world applications[2]. The most commonly used magnetic loss model is the

Steinmetz formula and its improved models, such as the modified Steinmetz formula (MSE), the generalized Steinmetz equation (GSE) and the improved GSE equation (iGSE)[3]. While equation-based magnetic loss modeling is easy to use, it cannot guarantee precise results across the entire application range.

Data-driven approaches have been considered as an effective means to surpass the limitations of equation-based magnetic loss modeling. Consequently, they have emerged as a prominent research focus in the field of magnetic loss modeling. The large scale magnetics material database - Magnet- has laid a solid foundation for data driven based magnetics material loss modeling[4]. [4] has proposed three types of neural network (NN) models for predicting core loss: scalar-to-scalar, sequence-to-scalar, and sequence-to-sequence models. The scalar-to-scalar NN model maps scalar inputs such as frequency, flux density, and duty ratio to a scalar output that represents core loss. The sequence-to-scalar NN model maps excitation waveforms to the core loss output. The sequence-to-sequence NN model maps flux density waveforms to magnetic field intensity waveforms and utilizes the B-H hysteresis loop to determine core loss. The scalar-to-scalar model has the smallest size, with a total of 1,594 parameters. However, it is only applicable for predicting losses under specific waveform shapes. The sequence-to-scalar model can handle different waveform shapes but does not incorporate temperature into the framework. On the other hand, the sequence-to-sequence model can handle all waveform shapes and temperature variations. However, it has the largest model size with 28,481 parameters, and the prediction bias in magnetic field intensity (H) can result in large core loss deviations. Existing research still has limitations in terms of model size, accuracy, and applicability range.

Therefore, a physics informed neural network (PINN) model with smaller size, higher accuracy, full applicability range and reduced data dependency is proposed. Firstly, an iGSE incorporated PINN model is established. By incorporating iGSE formula into the model, the acceleration of neural network training and mitigation of their reliance on extensive datasets have been achieved. Additionally, taking into account considerations of model size, accuracy, and applicability, we have chosen to adopt a neural network architecture that combines Gated Recurrent Unit (GRU) and Feedforward Neural Network (FNN). The GRU unit serves as an effective mechanism for processing sequential information, while the FNN unit is responsible for handling scalar information. This structure enables the integration of waveform, temperature, and frequency information within this

unified framework. To validate the effectiveness of our proposed approach, we have conducted repetitive experiments and evaluations. These evaluations include comparisons with PINN and normal NN, as well as the magnetics core loss NN model proposed by Princeton[4]. By considering various performance metrics, including accuracy, model size, and data size dependency, we can comprehensively assess the advantages and limitations of our proposed model.

II. MODELING OF PHYSICS INFORMED NEURAL NETWORK INCORPORATING IMPROVED GENERAL STEINMETZ EQUATION REQUIREMENTS

PINN has been widely used in the field of artificial intelligence, particularly in situations with limited data or when dealing with novel materials and operating condition. By integrating physical principles and constraints into the NN architecture, the PINN model leverages the available domain knowledge to guide the learning process. Therefore, PINN effectively improves the data utilization and thereby reducing the data dependency of neural networks.

The improved general Steinmetz equation (iGSE) is the most commonly used empirical formula for magnetic losses, which calculates core losses under arbitrary waveforms. The formula is shown in (1).

$$P_{iGSE} = \frac{k_i}{T} \int_0^T \left| \frac{1}{\Delta B} \frac{dB}{dt} \right| (\Delta B)^\beta dt$$

$$k_i = \frac{k}{(2\pi)^{\alpha-1} \int_0^{2\pi} |\cos \theta|^\alpha 2^{\beta-\alpha} d\theta} \quad (1)$$

Core loss of piecewise linear waveforms can be calculated as (2), in which ΔB_n and D_n are the change of magnetics flux density and duty cycle of each segment in a piecewise linear waveform. By calculating the integral in (2), the compact form for core loss of piecewise linear waveforms is shown in equation (3).

$$P_c = \frac{k_i}{T} \left[\int_0^{D_1 T} \left| \frac{1}{\Delta B_1} \frac{\Delta B_1}{D_1 T} \right|^\alpha (\Delta B_1)^\beta dt + \int_{D_1 T}^{(D_1+D_2)T} \left| \frac{1}{\Delta B_2} \frac{\Delta B_2}{D_2 T} \right|^\alpha (\Delta B_2)^\beta dt + \dots \right] \quad (2)$$

$$P_c = k_i \sum_n (\Delta B_n)^\beta D_n^{1-\alpha} f^\alpha \quad (3)$$

The logarithms of core loss for sinusoidal and piecewise linear waveforms are shown in equation (4) and (5) respectively.

$$\log P = \log k + \alpha \log f + \beta \log B \quad (4)$$

$$\log P = \log k_i + \alpha \log f + \log \left(\sum_n (\Delta B_n)^\beta D_n^{1-\alpha} \right) \quad (5)$$

Then gradient relationships between power loss P and frequency f, flux density B can be derived. Equation (6) and (7) shows gradient relationships between logP, logf, and logB for sinusoidal waveforms. For piecewise linear waveforms, the

gradient of logP with respect to logf is the same as Equation (6). Equation (8) shows gradient of logP with respect to $\log \Delta B_1$.

$$\frac{\partial \log P}{\partial \log f} = \alpha \quad (6)$$

$$\frac{\partial \log P}{\partial \log B} = \beta \quad (7)$$

$$\frac{\partial \log P}{\partial \log \Delta B_1} = \frac{D_1^{1-\alpha}}{D_1^{1-\alpha} (\Delta B_1)^\beta + D_2^{1-\alpha} (\Delta B_2)^\beta} \times \beta (\Delta B_1)^{\beta-1} \quad (8)$$

The iGSE formula is embedded in the neural network to assist in the learning process, as is shown in Fig. 1. The key is to use formula (6)-(8) to constrain the change of output with respect to the input, thereby determining the direction of parameter updates. The loss function of IGSE incorporated PINN is shown in equation (9)-(12). Equation (9) defines the residual1, which constrains the change of power loss with respect to frequency. Equation (10) and (11) defines the residual2 for sinusoidal and piecewise linear waveforms respectively, which constrains the change of power loss with respect to flux density. A smaller residual indicates that the updated direction of the output is more consistent with physical constraints.

$$residual_1 = \frac{\partial \log P}{\partial \log f} - \alpha \quad (9)$$

$$residual_2 = \frac{\partial \log P}{\partial \log B} - \beta \quad (10)$$

$$residual_2 = \frac{\partial \log P}{\partial \log \Delta B_1} - \frac{D_1^{1-\alpha} \beta (\Delta B_1)^{\beta-1}}{D_1^{1-\alpha} (\Delta B_1)^\beta + D_2^{1-\alpha} (\Delta B_2)^\beta} \quad (11)$$

$$loss = \frac{1}{N} \sum (\hat{P} - P)^2 + \frac{1}{N} residual_1^2 + \frac{1}{N} residual_2^2 \quad (12)$$

To verify the effectiveness of the PINN model, the normal NN model that has no embedded physics information is trained and tested for comparison. Repeating experiments are carried out while varying the amount of data for training. Fig. 2 shows the average relative errors of N87 material from MagNet Database, with different amount of data for training ranging from 25 to 1600. The error results are averaged over 10 trials to avoid randomness. The iGSE incorporated PINN has much lower relative error when the amount of data points available for training is small. This observation suggests that the integration of additional constraints from physical formulas in the PINN model facilitates faster learning and enhances the efficient utilization of data by the neural network. When the amount of data points for training reaches 1600, the PINN model and the normal NN model reaches the same average relative error at around 20%. As the training data becomes more abundant, it is possible for the performance of PINN to slightly lag behind that of traditional neural networks. This can be attributed to the errors introduced by incorporating physical constraints into the model.

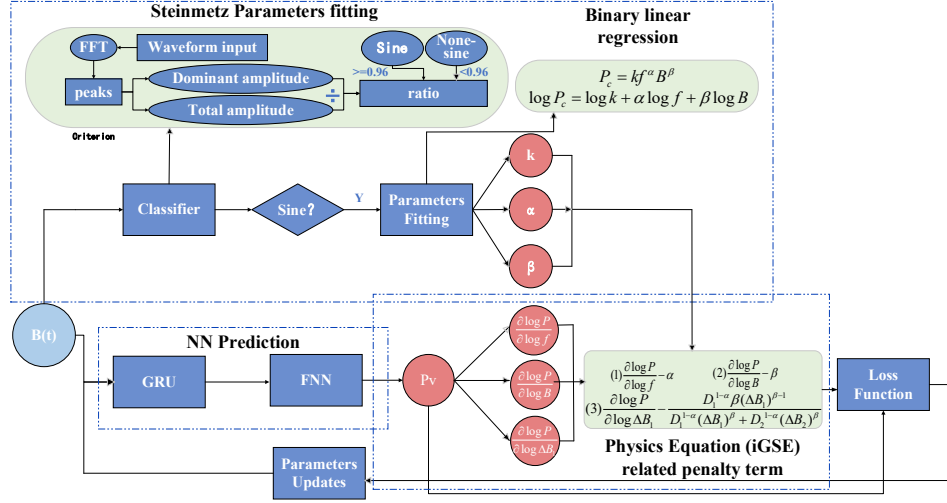


Fig. 1 IGSE incorporated PINN

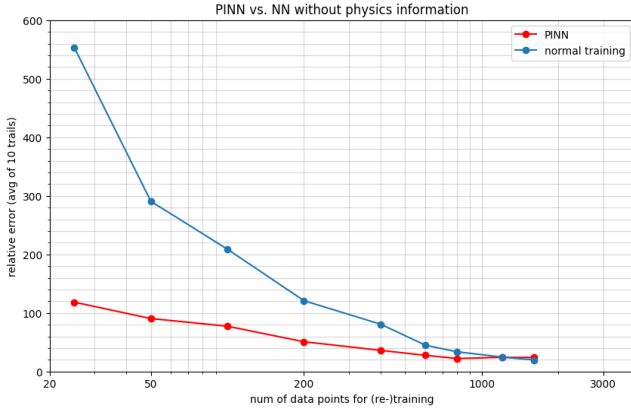


Fig. 2 Relative error of PINN and normal NN with a varied amount of training data

III. UNIFIED NN FRAMEWORK WITH SMALLER SIZE, HIGHER ACCURACY AND WIDE APPLICABILITY RANGES

The tradeoff between model size and accuracy is a crucial challenge in NN modeling, and an overall characterization of magnetics material loss behavior requires a unified framework. Therefore, a novel structure that enables the seamless integration of waveform, temperature, and frequency information should be constructed with compact size and high accuracy.

The proposed model should be able to handle sequential input flux density waveform $B(t)$, as well as multiple scalar inputs. The loss of magnetic materials is significantly affected by temperature, making it crucial to model the influence of temperature on the output loss accurately. To capture the temperature-dependent behavior of magnetic material loss, temperature T serves as a vital input for the proposed model. To incorporate physical information into the neural network, as mentioned in section 2, the proposed model utilizes formulas (9)-(12). This requires $\log f$, $\log B$ and the magnetic flux density variation value of the first segment of the

piecewise linear waveform ΔB_1 to be fed into the NN model as well. In summary, the proposed model should have two stages, to process sequential information $B(t)$, as well as scalar inputs T , $\log f$, $\log B$, and ΔB_1 .

GRU and LSTM are two widely used variants of recurrent neural networks (RNNs) that incorporates gating mechanisms, which renders the ability to handle time-series information. Compared to LSTM, GRU features a simpler gating mechanism comprising only an update gate and a reset gate. Consequently, GRU boasts fewer parameters and exhibits faster convergence. Hence, we opted for GRU as the network architecture for waveform processing. The GRU stage has 32 cell states and 32 hidden states. It takes the flux density waveform $B(t)$ as input, and the outputs are fed into FNN for further processing.

The FNN stage consists of one input layer, five hidden layers and one output layer that generates power loss prediction. The FNN aggregates the outputs of GRU stage and other four inputs, which are T , $\log f$, $\log B$ and ΔB_1 . The proposed model contains 4285 parameters in total. The overall structure of our proposed model is shown in Fig. 3.

The model is trained and tested under all types of waveforms and at all temperature conditions for N87 material, which contains 40616 data points in total. The prediction results have an average error of 1.36%, RMS error of 1.83%, and maximum error of 17.8%. The error distribution is shown in Fig. 4.

The same training process are also conducted on other materials provided in MagNet Database, including 3C90, 3C94, N27, etc., to verify the effectiveness of the proposed model. Fig. 5 shows the error histograms of 3C90 and 3C94, which contains 40713 and 40068 data points respectively.

Comparisons with the proposed PINN model and other existing models are summarized in TABLE I. It can be concluded that the proposed model reaches higher accuracy with a compact model size and wide applicable range.

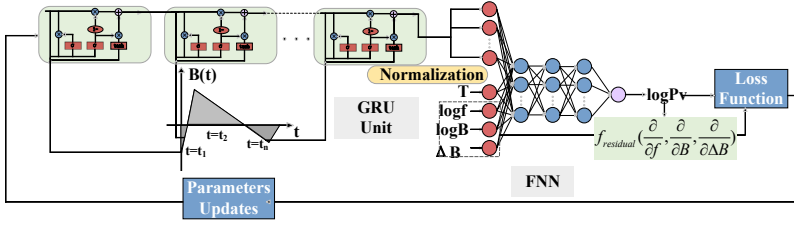


Fig. 4 The network structure of GRU based magnetic core loss modeling

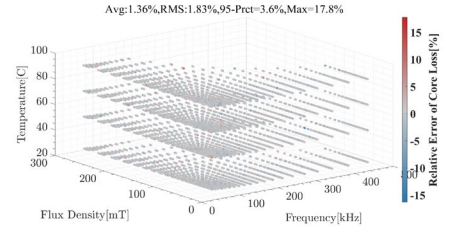


Fig. 3 Error distribution of N87 material prediction results under all types of waveforms and all temperature conditions

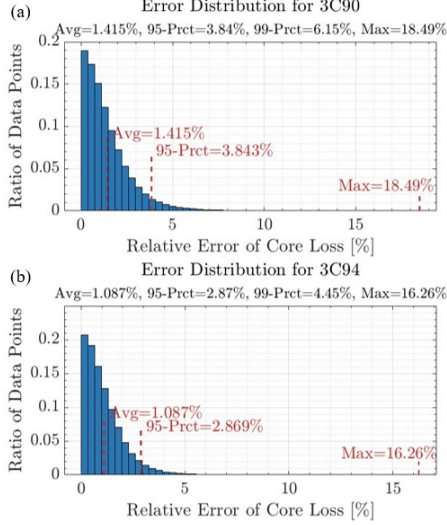


Fig. 5 (a) Error histograms of 3C90 (b) Error histograms of 3C94

IV. MODEL PERFORMANCE EVALUATION AND FINAL TEST RESULTS

To provide invaluable insights into a widely applicable training methodology for magnetics material modeling and deliver a meticulous evaluation of the model we put forth, we delved into the intricate technical aspects of the model training process and model evaluation. Additionally, exploration of the amount of data required for new material training is conducted as important part of our analysis. Finally, the 5 new materials are trained, and the evaluation of our proposed model in terms of mode size and accuracy are summarized.

A. Data Pre-processing and Model Training Method

Data pre-processing is the first and fundamental step for model training. For our proposed PINN model, it can be decomposed into mainly three steps:

(1) Sequence and scalar inputs and outputs processing: To minimize the impact of phase, and enhance the model's resilience to noise, a circular random phase shift is done on each magnetic density waveform, complemented by superposition with white noise. And frequency information is incorporated in the waveform by down sampling. To enhance the clarity of the input-output relationships, the output power loss, and input flux density, and frequency are logarithmically transformed.

(2) Classification of waveforms: This classification was accomplished by employing Fast Fourier Transform (FFT) to discern frequency components. Three waveform class—sinusoidal, triangular, and trapezoidal—are categorized and the change of magnetics flux ΔB , the duty cycles of each segment of piecewise linear waveforms D_n are recorded for later incorporation of formulas (9)-(12).

(3) Steinmetz parameters fitting: the classifier described in step (2) then passes the sinusoidal waveforms to the Steinmetz parameters fitting function, which employs the least squares method. This fitting process aims to estimate the Steinmetz parameters that characterize the magnetic properties of the material under consideration.

TABLE I
COMPARISONS WITH THE PROPOSED PINN MODEL AND OTHER EXISTING MODELS

Model	Model Size	Applicable Range	Test Condition		Error (%)
			Waveform Shape	Temperature	
Sequence-scalar[4]	5569	Handle only one temperature	tri.,	25°C	Avg: 2.09% Max: 14.35%
Sequence-sequence[4]	28481	Handle all waveforms and all temperature	Sine, tri., trape.	25°C, 50°C, 70°C, 90°C,	Avg: 4.2% Max: 30%
Proposed PINN model	4285	Handle all waveforms and all temperature	Sine, tri., trape.	25°C, 50°C, 70°C, 90°C,	Avg: 1.36% Max: 17.8%

Due to the limited training dataset available for new materials, we applied k-fold training to maximize the utilization of the dataset for neural network training. The training dataset is randomly split into training and test set as 80% and 20%. Then use k-fold training to further divide the first part into k subsets, with one subset serving as the validation set and the remaining k-1 subsets used for training during each iteration. Under the considerations of available data quantity and computational resources, the decision has been made to use k=5 for training. Therefore, thorough evaluation on the model's performance can be conducted and the most suitable model that achieves the best overall performance across the five folds can be chosen.

MagNet database has provided abundant magnetism loss data for materials including N87, N49, 3C90, etc, which provides basis for new material training. During the initial stages of the competition, we trained the magnetic loss model using a substantial amount of data, which serves as a valuable starting point for training new materials. In order to assess the model's ability to generalize, we conducted zero-shot experiments by directly testing the pre-trained N87 material loss model on material A. The results demonstrated that the model captured some knowledge about the loss mechanism and the factors that influence it, while due to the inherent differences between materials, the zero-shot errors were large and further training needs to be conducted. Subsequently, normal training and transfer learning are conducted. Transfer learning uses the pretrained model as a start point and re-trains with the new material data, while normal training uses randomly initialized neural network. Transfer training provides better accuracy results, which verifies the effectiveness of the pre-trained model as a starting point for training new materials. leveraging the knowledge acquired from the previous training. TABLE II summarizes the zero-shot, normal training, and transfer learning results on material A, testing on a same test set and the error results are averaged over 10 trials to avoid randomness and for better comparison.

B. Data Dependency Exploration

The neural network performance dependency on the amount of data are explored, to give valuable insights into determining the minimum amount of data required to achieve an acceptable error level during training. The figure shows the relative error results of material A with varying amount of data for training. The proposed PINN model is compared with normal NN model that doesn't incorporate physics formula. Repetitive experiments are conducted with different amount of data for training ranging from 25 to 2400, and the error results are averaged over 10 trials to avoid randomness.

TABLE II
ZERO-SHOT, NORMAL TRAINING AND TRANSFER LEARNING
RESULTS OF MATERIAL A

Error	Zero-shot	Normal training	Transfer learning
Avg. Relative Error	35.89	10.52	7.46
RMS Relative Error	41.89	15.50	10.77
Max Relative Error	137.08	116.12	85.61

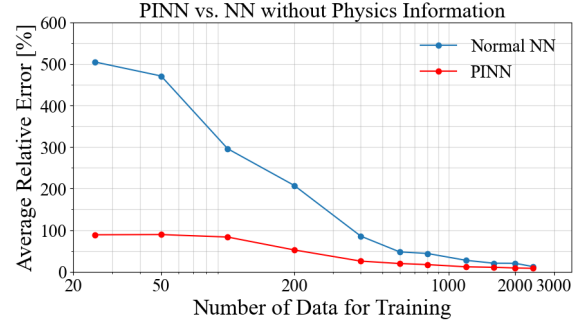


Fig. 6 Data dependency results of normal NN and PINN for material A

Remarkably, the model exhibits reduced data dependency, as it achieves comparable accuracy with just 25 data points, whereas normal NN model that doesn't incorporate physics information require more than 300 data points for acceptable performance. The results show the proposed PINN model helps enhance the effective utilization of data by neural networks. These findings provide crucial insights into determining the optimal amount of data necessary for training to achieve an acceptable error level. By understanding the data dependency, researchers and practitioners can make informed decisions regarding the dataset size and allocation, ultimately enhancing the overall performance and efficiency of the neural network model.

C. Final Evaluation Results

Using our proposed model, we successfully obtained the final results for the 5 new materials. The model size and accuracies are summarized in TABLE III.

The model demonstrated promising accuracy for Materials A, B, C, and E, with relatively low average and 95% percentile errors. However, the accuracy for Material D was comparatively lower, with higher errors.

To improve the accuracy for Material D and enhance overall performance, further analysis is needed to identify the specific reasons behind the lower accuracy. Possible improvements could include acquiring additional data for Material D, refining the data pre-processing steps, or exploring alternative model architectures.

In conclusion, our study developed a training methodology for magnetic material modeling and evaluated the proposed model on 5 new materials. The results showcased the effectiveness of our approach, although further enhancements are required for certain materials. The insights gained from data dependency analysis can guide researchers in determining optimal data sizes for training, leading to improved neural network performance and efficiency.

TABLE III
TEST RESULTS OF 5 NEW MATERIALS

Material	Model Size	Accuracy
Material A	4285	Avg:2.90%, 95-prct: 8.08%
Material B		Avg:1.47%, 95-prct: 4.04%
Material C		Avg:3.17%, 95-prct: 8.44%
Material D		Avg:8.04%, 95-prct: 23.27%
Material E		Avg:2.99%, 95-prct: 8.85%

REFERENCES

- [1] McLyman C W T. Transformer and inductor design handbook[M]. CRC press, 2016.
- [2] Mühlethaler J. Modeling and multi-objective optimization of inductive power components[D]. ETH Zurich, 2012.
- [3] Z. Li, W. Han, Z. Xin, Q. Liu, J. Chen and P. C. Loh, "A Review of Magnetic Core Materials, Core Loss Modeling and Measurements in High-Power High-Frequency Transformers," in CPSS Transactions on Power Electronics and Applications, vol. 7, no. 4, pp. 359-373, December 2022, doi: 10.24295/CPSSPEA.2022.00033.
- [4] H. Li, S. R. Lee, M. Luo, C. R. Sullivan, Y. Chen and M. Chen, "MagNet: A Machine Learning Framework for Magnetic Core Loss Modeling," 2020 IEEE 21st Workshop on Control and Modeling for Power Electronics (COMPEL), Aalborg, Denmark, 2020, pp. 1-8, doi: 10.1109/COMPEL49091.2020.9265869.